BMC Plant Biology

RESEARCH

Open Access

Genome-wide identification and expression analysis of glutaredoxin in *Puccinellia tenuiflora* under salinity stress

Yanshuang Liu[1,2†], Xia Han[2†], Juanjuan Yu[3], Yueyue Li[1,2], Meihong Sun[2], Qiuying Pang[1], Ying Li[1*] and Shaojun Dai[2*]

Abstract

Background Glutaredoxins (GRX) are key oxidoreductases that modulate protein redox states during plant development and stress responses. Alkaligrass (*Puccinellia tenuiflora*) is a highly salt-tolerant forage grass, but its *GRX* gene family (PutGRXs) remains uncharacterized, unlike those in Arabidopsis and other plants.

Results We identified 25 *PutGRX* genes in the *P. tenuiflora* genome. Phylogenetic analysis revealed close evolutionary ties to monocotyledonous rice (*Oryza sativa*). Based on gene structure and conserved domains, *PutGRXs* were classified into three groups: five CGFS-type, eleven CPYC-type, and nine CC-type GRXs. Promoter analysis identified numerous *cis*-acting elements linked to abiotic stresses (e.g., light, drought, heat, cold) and hormone responses, suggesting a pivotal role in stress adaptation. Tissue-specific expression profiling showed differential *PutGRX* expression in roots, leaves, stems, flowers, and sheaths, with most genes responding to NaCl, $NaHCO_3$, and Na_2CO_3 stresses. Functional characterization of chloroplast-localized PutGrxS12 demonstrated its importance in plant growth and ROS scavenging under salinity stress.

Conclusion This study offers the first comprehensive genomic and functional analysis of the *PutGRX* family in *P. tenuiflora*, highlighting its conservation, classification, and stress-responsive roles. Our findings advance understanding of GRX-mediated stress tolerance and provide potential targets for engineering salt-resistant crops.

Keywords Glutaredoxins (GRX) gene family, Expression profiling, Abiotic stress, *PutGrxS12*, *Puccinellia tenuiflora*, Salt tolerance

Introduction

Alkaligrass (*Puccinellia tenuiflora*) is a monocotyledonous halophyte widely distributed in China's Songnen Plain. This species demonstrates exceptional salt-alkali tolerance, surviving under extreme conditions of 600 mM NaCl and 150 mM Na_2CO_3 (pH 11.0) [1]. As a pioneer species in saline environments, alkaligrass serves both as a valuable pasture for soil remediation and as a model organism for studying alkali tolerance mechanisms.

The recently assembled chromosome-level genome of *P. tenuiflora* (1.50 Gb) encodes 38,387 protein-coding genes and contains 54.9% transposable elements, primarily long terminal repeats [2]. Comparative genomic

†Yanshuang Liu and Xia Han contributed equally to this work.

*Correspondence:
Ying Li
Ly7966@163.com
Shaojun Dai
daishaojun@shnu.edu.cn
[1] Key Laboratory of Saline-Alkali Vegetation Ecology Restoration (Northeast Forestry University), Ministry of Education, College of Life Sciences, Northeast Forestry University, Harbin 150040, China
[2] Development Center of Plant Germplasm Resources, College of Life Sciences, Shanghai Normal University, Shanghai 200234, China
[3] College of Life Sciences, Henan Normal University, Xinxiang 453007, China

and transcriptomic analyses have uncovered thousands of salinity-responsive genes in this halophyte [2]. Quantitative proteomic studies have systematically quantified stress-induced alterations in protein abundance and post-translational modifications under diverse conditions including salt stress (NaCl, Na_2CO_3, and $NaHCO_3$), low temperature, and oxidative stress [3–10]. Integrative multi-omics analyses demonstrate that *P. tenuiflora* employs unique adaptive strategies for salinity tolerance, particularly through the dynamic regulation of its sophisticated reactive oxygen species (ROS) scavenging antioxidant systems [3, 11].

Salinity stress triggers excessive ROS production, inducing oxidative damage that compromises cellular integrity and protein function. This oxidative stress promotes modifications of reactive protein thiol groups, including sulfenylation (protein-SOH), S-nitrosylation (protein-SNO), and S-glutathionylation (protein-SSG). The glutathione/glutaredoxin (GSH/GRX) system plays a crucial role in maintaining protein redox homeostasis under these conditions, serving as a key regulatory mechanism for stress adaptation [12].

Glutaredoxins (GRXs) are multifunctional proteins involved in iron-sulfur (Fe-S) cluster assembly and protein redox regulation [13–15]. The GRX family varies in size across species: ~30 members in higher plants [16], six in the green algae *Chlamydomonas reinhardtii* [17], and three in the cyanobacterium *Synechocystis* spp [18]. Land plants (including bryophytes) possess three GRX subclasses defined by active-site motifs: CGFS-, CPYC- and CC- types [16]. The CGFS-type GRXs feature a conserved CGFS motif enabling $[Fe_2S_2]$ cluster binding and transfer, though they lack oxidoreductase activity [19]. Chloroplastic GrxS14/S16, homologous to bacterial/yeast/human GRXs, form $[Fe_2S_2]$-bridged heterodimers with BolA proteins and deliver clusters to SufA1 and ferredoxin (FDX) [20]. Mitochondrial AtGrxS15 (essential for embryogenesis) and cytosolic AtGrxS17 (regulating heat tolerance) also bind $[Fe_2S_2]$ clusters [21, 22]. CPYC-type GRXs (C[P/S]Y[C/S] motif) exhibit oxidoreductase activity and are represented by *Escherichia coli* Grx1/3 [23], yeast GRX1/2 [24], and mammalian GRX1/2 [25]. In plants, *Populus trichocarpa* PtGrxS12 (CSYS motif) and *Arabidopsis thaliana* AtGrxS12 (CSYC motif) regulate substrate redox via deglutathionylation (e.g., PtA4-GAPDH, AtMSRB1) [13, 26–28]. Unlike PtGrxS12, AtGrxC5 forms $[Fe_2S_2]$ homodimers [13, 26]. The CC-type GRXs (CC[M/L][C/S/G/A/I] motif) are plant-specific and function in development (e.g., ROXY19 in petal morphogenesis [29], detoxification [30], and salicylic acid (SA)- or jasmonic acid (JA) -mediated disease resistance [31, 32]. ROXY11–13 and ROXY15 additionally modulate nitrate-responsive primary root growth [33].

In this study, we identified 25 *PutGrx* genes in *Puccinellia tenuiflora* through genome-wide screening. We analyzed their phylogenetic relationships, chromosomal distribution, gene structures, conserved functional domains, and subcellular localization. Furthermore, we characterized *PutGRX* expression patterns across different tissues and under various salinity stress conditions. Phenotypic and physiological analyses of Arabidopsis *atgrxs12* mutants and *PutGrxS12*-overexpressing lines demonstrated that *PutGrxS12* plays an essential role in plant growth and ROS scavenging during salt stress adaptation.

Materials and methods

Identification and cloning of *PutGRX* genes in *Puccinellia tenuiflora*

To determine the GRX family of alkaligrass, we downloaded the genome from the genomic data of *Puccinellia tenuiflora* (http://www.xhhuanglab.cn/data/alkaligrass.html). We used 31 AtGRX protein sequences from Arabidopsis as queries to search the *Puccinellia tenuiflora* genome database using BLASTp, setting a cutoff value of $1E^{-100}$ for the expected value (*e*-value). To confirm the conserved domain, we submitted the candidate PutGRXs to the NCBI web CD-search tool (https://www.ncbi.nlm.nih.gov/Structure/bwrpsb/bwrpsb.cgi). The coding sequences (CDSs) and protein sequences of PutGRXs were displayed in Supplemental Table S1 and S2.

Phylogenetic analysis of GRXs from different plant species

The phylogenetic tree of GRXs in alkaligrass and three other plant species including Arabidopsis, rice (*Oryza sativa*), and poplar (*P. trichocarpa*) were constructed with MEGA-X by the neighbor- joining (NJ) method and 1,000 bootstrap replicates. The protein sequences of 31 Arabidopsis AtGRXs [16], 28 rice OsGRXs and 38 poplar PtGRXs [34] have been reported previously.

Chromosomal distribution of *PutGRX* genes

The positional information of the *PutGRX* genes on the chromosome were obtained from the Alkaligrass Base (http://www.xhhuanglab.cn/data/alkaligrass.html). The chromosome distribution, length, and the start and end positions were visualized using MapGene2 Chrom web v2 (http://mg2c.iask.in/mg2c_v2.0/).

Collinearity analysis of *GRXs* between alkaligrass and other plants

The collinearity analysis of *GRXs* between the Arabidopsis, rice, and poplar homologs was verified and visualized

using One Stem MCScanX and Dual Systeny Plot for MCScanX in TBtools software, respectively.

Analyses of gene structure and conserved motif of PutGRXs

The exon–intron structure was examined using TBtools, based on the genomic sequence and CDS of each *PutGRX*. The conserved motifs of PutGRXs (with a maximum of 15 motifs) were identified by MEME (https://meme-suite.org/meme/tools/meme) and visualized with TBtools.

Identification of putative cis-regulatory elements in *PutGRXs* promoters

The promoter sequences (2,000 bp before the start codon) of all *PutGRXs* were extracted from the alkaligrass Base (http://www.xhhuanglab.cn/data/alkaligrass.html), and were analyzed by using the PlantCARE (http://bioinformatics.psb.ugent.be/webtools/plantcare/html/) tool and visualized by TBtools.

Plant materials and RT-qPCR analysis

The seeds of *Puccinellia tenuiflora* were collected from the AnDa Experimental Base of the Alkali Soil Natural Environmental Science Center, Northeast Forestry University (AnDa, China). Alkaligrass seedlings were grown in a modified Hoagland's solution under controlled conditions of 25 °C and 75% relative humidity. The seedlings were exposed to 300 μmol m^{-2} s^{-1} of light for 13 h, followed by 11 h of darkness, on a daily basis for a period of 30 days [3].

For the tissue organ expression analysis of *PutGRXs*, three-week-old alkaligrass seedlings were subjected to a modified Hoagland's solution comprising 50 mmol L^{-1} Na_2CO_3, 100 mmol L^{-1} NaCl, and 100 mmol L^{-1} $NaHCO_3$ (pH 9.0) for 24 h, respectively. The leaves and roots were harvested immediately after the treatments, frozen in liquid nitrogen, and stored at − 80 °C for future analysis.

The RNA was extracted from the alkaligrass leaves using TRIzol™ LS reagent (Invitrogen, USA). Genomic DNA was eliminated through DNase treatment of total RNA, which was subsequently reverse transcribed into cDNA using the PrimeScript RT kit (Takara, Japan). For RT-qPCR analysis, the SYBR Premix ExTaq II kit (TRAN, China) was used with *PutActin* serving as an internal control. The primer pairs used were specifically designed through the Primer3 Web tool (http://bioinfo.ut.ee/primer3/) (Supplemental Table S3). RT-qPCR analyses were performed using three independent biological replicates, and the data were normalized using the $2^{-\Delta\Delta Ct}$ method [35].

Prediction of the Subcellular Localization of PutGRXs

The subcellular localizations of 25 PutGRX proteins were predicted using four online analysis tools, the URLs of which are given below, along with the screening criteria for credible localization results. (1) Plant-mPLoc (http://www.csbio.sjtu.edu.cn/bioinf/plant-mμLti/) tool does not require screening parameter, and the output results are credible localization prediction results. (2) iPSORT Prediction (https://ipsort.hgc.jp/) does not require screening parameters, and the output results are the credible positioning prediction results. (3) WoLF PSORT (https://wolfpsort.hgc.jp/) requires the'nearest neighbors'parameter to be ≥ 5 in order to achieve a plausible localization prediction result. (4) TargetP- 2.0 (http://www.cbs.dtu.dk/services/TargetP/) prediction results are deemed credible if the 'reliability class' is ≤ 3.

PutGRX protein 3D structure prediction

The AlphaFold database was utilized to predict the 3D structure of the PutGRX protein. The automatic modeling mode was selected in the analysis interface of AlphaFold database. The predicted 3D structures of proteins were visualized using Pymol software.

Subcellular localization of PutGrxS12

The open reading frame of PutGrxS12 and its three cysteine mutations ($PutGrxS12^{C78S}$, $PutGrxS12^{C136S}$ and $PutGrxS12^{C78S/C136S}$) were inserted into the plant expression vector pCAMBIA1300-*GFP*, resulting in the production of a PutGrxS12 fusion protein under the control of CaMV 35S promoter. The derived plastids of pCAMBIA1300-*PutGrxS12-GFP* and the empty vector pCAMBIA1300-*GFP* were transferred into Arabidopsis protoplasm cells, respectively. Protoplasts were isolated from Arabidopsis leaves via enzymatic digestion using cellulase (Yakult, Japan) [36]. The resulting GFP signals in these cells were visualized using an Olympus FV3000 confocal laser scanning microscope (Olympus, Japan). The subcellular localization of PutGrxS12 in these cells was subsequently determined by the observation of the GFP green fluorescence signals, in conjunction with their merged images displaying chlorophyll fluorescence and bright field signals.

Vector construction and plant transformation

The pCAMBIA1300-GFP plasmid was subjected to double enzymatic cleavage (BanHI and XbaI). The target CDS fragment was prepared using alkaligrass cDNA as a template, and the pCAMBIA1300-GFP vector was then ligated with the *PutGrxS12* gene fragment by homologous recombinase at 37℃ for 30 min. The recombinant product was then transformed into DH5α *E. coli*. The

sequenced monoclonal positive strain was then transformed into EH105 for expression. *Agrobacterium tumefaciens* strain EHA105 cells containing the pCAMBIA1300-*PutGrxS12*-GFP plasmid were transformed into Arabidopsis WT seedlings by the floral dip method to obtain *PutGrxS12*-overexpressed seedlings. The transformed seedlings were screened on 1/2 MS agar medium containing 40 μg/mL Hygromycin, and the *PutGrxS12* levels were subsequently assessed in several independent homozygous T3 strains by RT-qPCR with gene-specific primers (Supplemental Table S3).

Salinity tolerance analysis of *PutGrxS12* transgenic Arabidopsis

The T-DNA insertion mutant Arabidopsis *grxs12* (SALK_121961 C) was purchased from Arashare Science (https://www.arashare.cn/index). The homozygous mutant plants were identified through PCR-based genotyping. The primers used in this study are listed in Supplementary Table S3. The WT, *atgrxs12* mutant, and *PutGrxS12*-overexpressed Arabidopsis seedlings were cultivated for four weeks. The four-week-old Arabidopsis seedlings were used for phenotypic observation. We quantified the area of the seventh and eighth leaves and inflorescence length in four-week-old plants. Four-week-old plants subsequently treated with 150 mmol L^{-1} NaCl for a period of nine days in a light incubator (22 °C 16 h of light/20 °C 8 h of darkness, 65% relative humidity). Photographs were taken after treatment.

Staining assay of superoxide anion ($O_2 \cdot^-$)

The accumulation of $O_2 \cdot^-$ in the leaves from the plants was detected by the NBT staining methods according to the previous methods [7]. Excised leaves were immersed in tubes containing fresh NBT staining solutions overnight in the dark. For proper visualization of the staining, the leaves were immersed in absolute ethanol to remove chlorophyll and then boiled for 10 min. The leaves were then placed in 10% glycerol and were photographed using a stereomicroscope [7].

Results

Comparative phylogenetic analysis of GRXs in alkaligrass and model plants

An un-rooted phylogenetic tree was constructed to explore the evolutionary relationships between alkaligrass GRXs (PutGRXs) and their orthologs in with other proteins. The protein sequences of 25 PutGRXs, 31 GRX from Arabidopsis (*A. thaliana*) [16], 28 from rice (*Oryza sativa*) [37], and 38 from poplar (*P. trichocarpa*) [34] were utilized to construct the phylogenetic tree. The 25 PutGRX sequences were retrieved from the alkaligrass genome database using BLASTp searches. Among these, twelve *PutGRX* genes were experimentally cloned and sequenced from alkaligrass genomic DNA. Sequence verification revealed errors in four genes (*PutGrxC2*, *PutROXY5*, *PutROXY7*, and *PutROXY8*) from the genome database, which were subsequently corrected (Supplemental Table S1). The remaining 97 reference GRX sequences from Arabidopsis [16], rice [37], and poplar [34] were obtained from previously published studies.

A total of 122 GRXs were categorized into four groups: 30 CPYC-type, 19 CGFS-type, 40 CC-I-type, and 33 CC-II-type (Fig. 1A). Among the 25 PutGRXs identified in alkaligrass, 11 were CPYC-type, five were CGFS-type, and nine were CC-I-type, with no PutGRXs belonging to the CC-II-type (Fig. 1A). Phylogenetic analysis revealed that GRXs are highly conserved between monocotyledonous and dicotyledonous plants. Most alkaligrass PutGRXs showed strong sequence similarity to rice OsGRXs within each group, with nine PutGRXs and 16 OsGRXs clustering together in the CC-I-type subgroup (Fig. 1A). The CC-type GRXs are characterized by a conserved CC[M/L][C/S/G/A/I] motif, which appears to be exclusive to land plants. Further studies are needed to determine whether monocot-specific CC-type GRXs have specialized functions. Sequence analysis demonstrated that all 11 CPYC-type GRXs contain the canonical C[P/S]Y[C/S] active site, essential for oxidoreductase activity. Similarly, the five CGFS-type GRXs possess a conserved CGFS motif, likely involved in $[Fe_2S_2]$ cluster binding and translocation.

Chromosomal distribution analysis of *PutGRXs*

Chromosome distribution analysis revealed that 25 *PutGRXs* exhibited an uneven and non-random distribution across the seven chromosomes in alkaligrass (Fig. 2A). Chromosome 6 harbored eight *PutGRXs*, while chromosomes 5 and 7 each contained four *PutGRXs*, and chromosome 3 had three *PutGRXs*, with chromosomes 1 and 2 each having two *PutGRXs* (Fig. 2A). The distribution of CPYC-type *GRXs* was localized across chromosomes 1 to 6, while CGFS-type *GRXs* were exclusively present on chromosomes 1, 5, and 7. Notably, the distribution of CC-type *GRXs* was confined to chromosomes 6 and 7, suggesting a potential specific association with these particular chromosomes (Fig. 2A).

Collinearity analysis of *GRXs* between alkaligrass and other plants

A collinearity analysis was performed to make a comparison between the homologous *GRX* genes in alkaligrass, Arabidopsis, poplar, and rice (Fig. 2B). The results revealed that alkaligrass *PutGRXs* had one, five, and 19 homologous gene pairs in Arabidopsis, poplar, and rice,

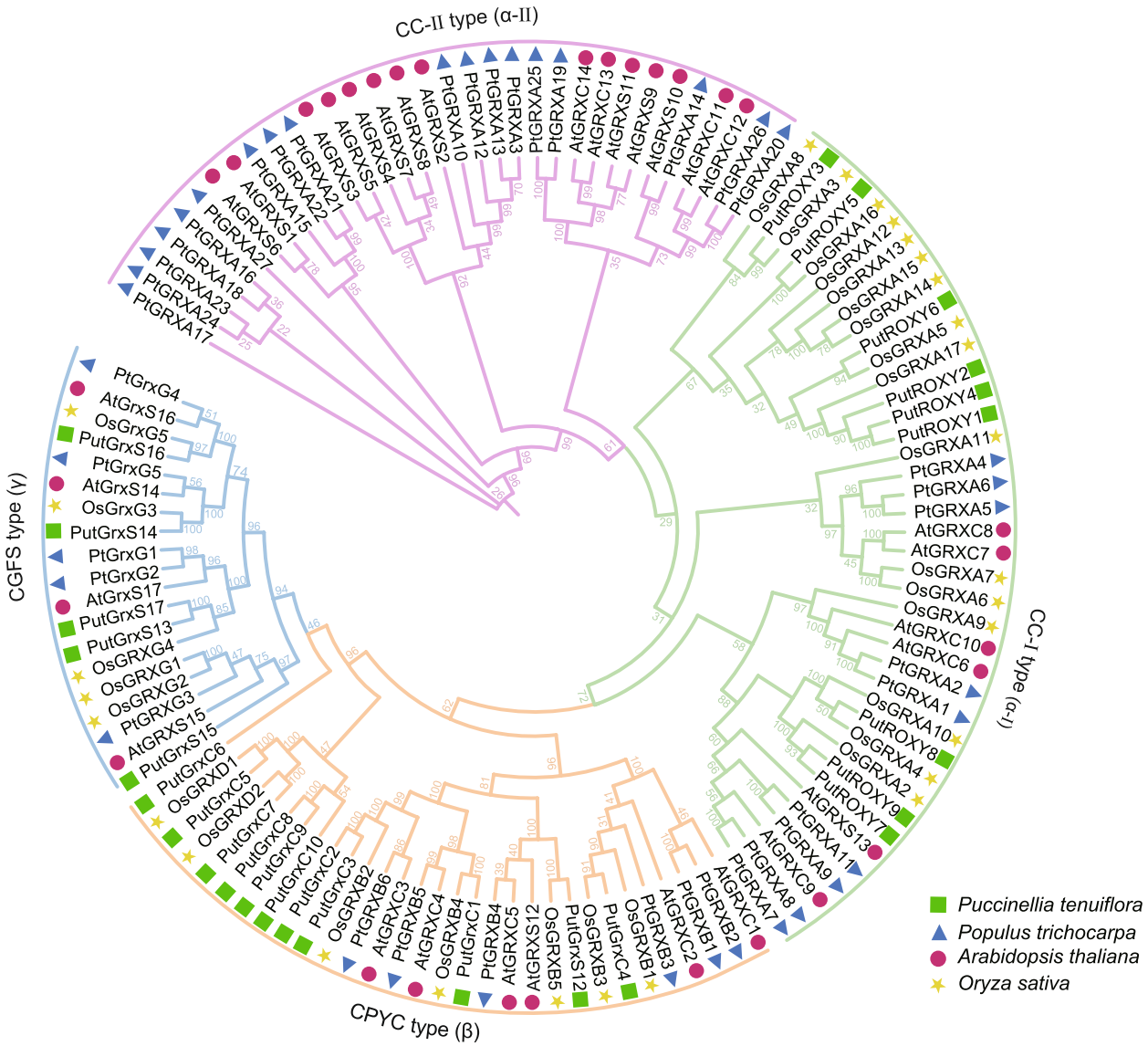

Fig. 1 Phylogenetic analysis of glutaredoxin (Grx) from *Puccinellia tenuiflora* and three other representative plants. The phylogenetic tree was built based on the amino acid sequences of the Grxs by MEGA4-X with the maximum likelihood method, which indicated the phylogenetic relationships among 122 GRXs from alkaligrass (*Puccinellia tenuiflora*), poplar (*Populus trichocarpa*), *Arabidopsis thaliana*, and rice (*Oryza sativa*). The colored ranges indicated the total Grxs proteins classed into four distinct categories: CPYC-type, CGFS-type, CC-I type, and CC-II type. The CC-type, CPYC-type and CGFS-type correspond to the alpha, beta, and gamma groups, respectively, as designated by Xu et al. [32] in their nomenclature. Various shapes represented different plant species. The accession numbers, coding sequences (CDSs), and amino acid sequences of the Grxs were listed in Supplemental Table S1 and S2. Bootstrap = 1000

respectively (Fig. 2B). Among them, alkaligrass *PutGrxC9* (Put_Chr0601903) exhibited conserved synteny across all four species. Furthermore, *PutGrxS13* and *PutGrxS17* demonstrated particularly close linkage with rice *OsGrxG4* (Os10g35720). These findings indicate that alkaligrass *GRX* genes share stronger phylogenetic relationships with rice orthologs than with other species, and certain *PutGRX* members (particularly *PutGrxC9*) exhibit exceptional evolutionary conservation (Supplemental Table S4) (Fig. 2B).

To investigate gene duplication events in the *PutGRXs* family, a covariance analysis was conducted using MCScanX. This analysis identified three highly homologous gene pairs (*PutGrxC2/PutGrxC3*, *PutGrxC8/PutGrxC9*, and *PutROXY5/PutROXY4*) that exhibited high levels of homozygosity, with sequence identity of 98.45%, 55.50%, and 90.82%, respectively. In addition, the

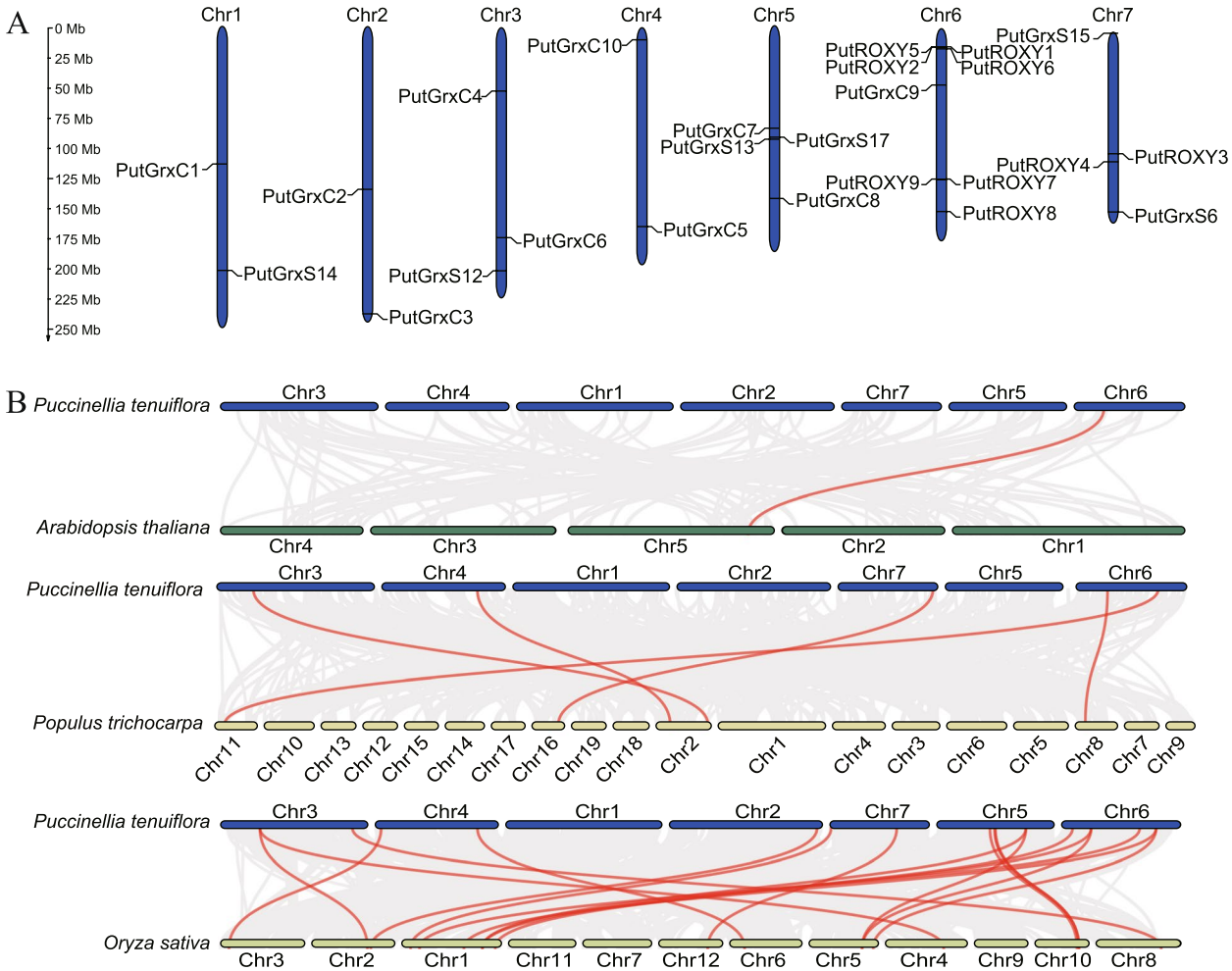

Fig. 2 Distribution of *PutGRXs* on chromosomes and collinearity analysis of *GRXs* between *Puccinellia tenuiflora* and other plant species. **A** Distribution of *PutGRXs* on chromosomes. The diagram was drawn using the MapGene2 Chrom web v2 tool. 25*PutGRXs* genes were located on seven chromosomes. The vertical bars marked the chromosomes of *P. tenuiflora*. The scale on the left represented the chromosome length. **B** Collinearity analysis of *GRXs* among alkaligrass (*P. tenuiflora*), poplar (*Populus trichocarpa*), *Arabidopsis thaliana*, and rice (*Oryza sativa*). Gray lines in the background indicated the collinear blocks within *P. tenuiflora* and other plant genomes, while the red lines highlighted the syntenic *Grx* gene pairs

non-synonymous substitution rate (Ka) over the synonymous substitution rate (Ks) (Ka/Ks values) of these gene pairs were less than 1 (Supplemental Table S5). These findings demonstrate that these gene pairs originated through segmental duplication events and subsequently experienced strong purifying selection, indicating functional constraints on their protein-coding sequences [38].

Gene structure and protein function domain analysis of PutGRXs

The PutGRXs were categorized into three distinct groups (CC-type, CPYC-type, and CGFS-type) based on their amino acid sequences. The CC-type GRXs comprised nine GRXs from PutROXY1 to PutROXY9, the CPYC-type GRXs encompassed 11 GRXs from PutGrxC1 to PutGrxC10 and PutGrxS12, while the CGFS-type GRXs included five GRXs from PutGrxS13 to PutGrxS17 (Fig. 3A).

To predict the evolutionary features and functional diversification of *PutGRXs*, the exon–intron organization of 25 *PutGRX* was analyzed. All the CC-type *GRXs* and three CPYC-type *GRXs* (*PutGrxC8*, *PutGrxC9*, and *PutGrxC10*) lack 5'UTR and 3'UTR (Fig. 3B). In contrast, three CGFS-type *GRXs* (*PutGrxS14*, *PutGrxS15*, *PutGrxS16*) and CPYC-type *PutGrxC7* have only 3'UTR (Fig. 3B). The remaining seven CPYC-type *GRXs* (from *PutGrxC1* to *PutGrxC6* and *PutGrxS12*) and two

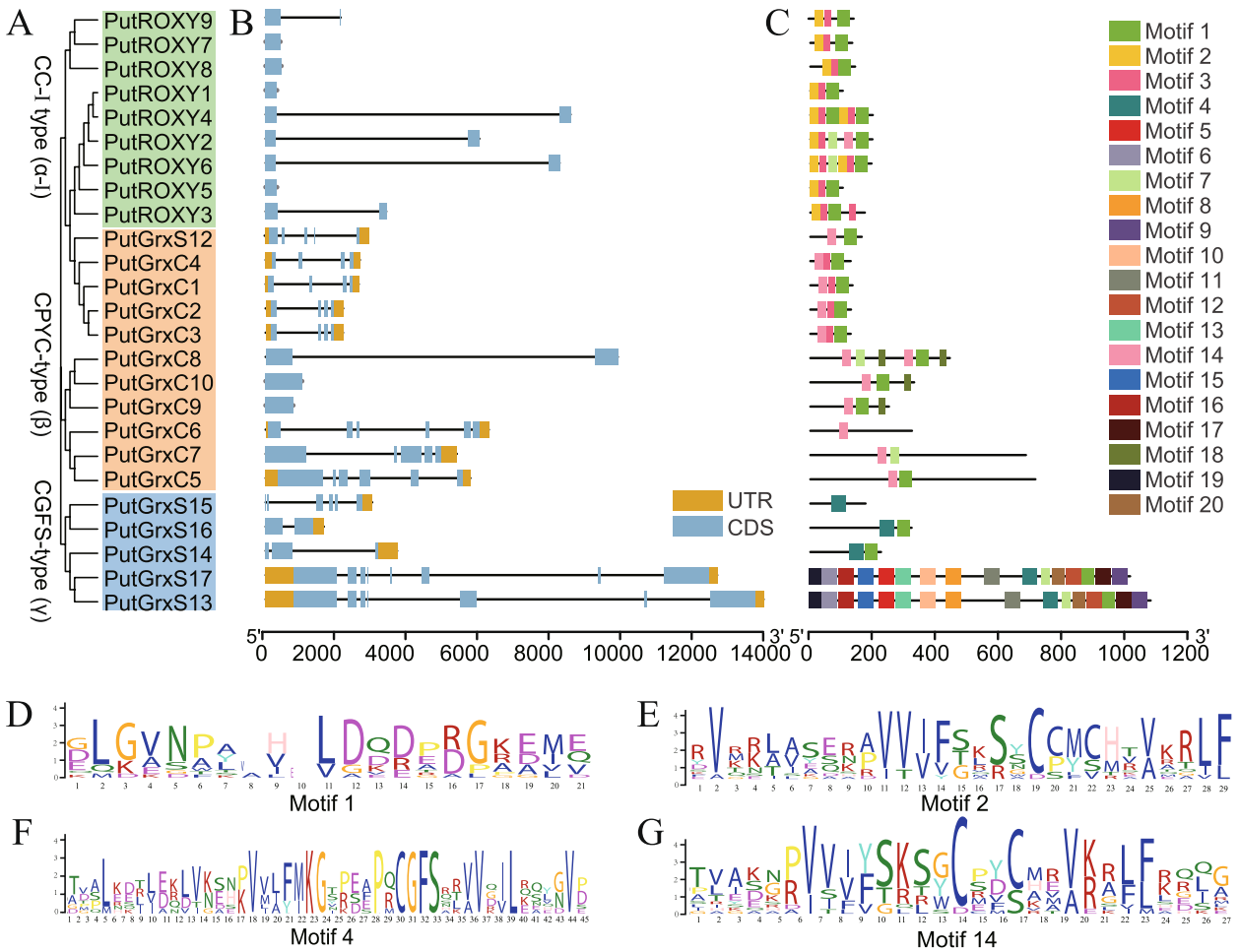

Fig. 3 Phylogenetic tree, gene structure and conserved motifs of PutGRXs. **A** Phylogenetic tree of PutGRXs constructed by the Neighbor-Joining method. **B** The structure of *PutGRXs* include exons, introns, and untranslated regions (UTRs). Yellow boxes indicated UTR, Yellow boxes indicate untranslated regions, light blue boxes indicate exons, and lines indicate introns. **C** Conserved motifs in PutGRXs. Different colors represent different motifs. **D-G** The logos showing the conserved residues in motif 1 (**D**), motif 2 (**E**), motif 4 (**F**), and motif 14 (**G**)

CGFS-type *GRXs* (*PutGrxS13* and *PutGrxS17*) possess both 5'UTR and 3'UTR (Fig. 3B).

Four CC-type *GRXs* (*PutROXY1*, *PutROXY5*, *PutROXY7* and *PutROXY8*) and two CPYC-type *GRXs* (*PutGrxC9* and *PutGrxC10*) contain only one exon (Fig. 3B). Conversely, five CC-type *GRXs* (*PutROXY2*, *PutROXY3*, *PutROXY4*, *PutROXY6*, and *PutROXY9*), CPYC-type *PutGrxC8*, and CGFS-type *PutGrxS16* possess two exons, while the remaining 12 *PutGRXs* exhibit multiple exons (Fig. 3B). The observed diversity of introns and exons suggests that alternative splicing in *PutGRXs* is likely to be important for GRX functions in regulating alkaligrass development and stress responses.

Conserved motif analysis revealed that 20 different motifs were unevenly distributed across the 25 PutGRXs (Fig. 3C). Motif 1 was the most conserved motif, being present in 24 PutGRXs with the exception of PutGrxS15 (Fig. 3D). Importantly, motif 2, motif 14, and motif 4 contain the conserved amino acid sites belonging to the CC-type, CPYC-type, and CGFS-type PutGRXs, respectively (Fig. 3E, F and G). In the CGFS-type GRXs, PutGrxS15 has only motif 4, PutGrxS14 and PutGrxS16 have motif 1 and motif 4, while PutGrxS13 and PutGrxS17 contain 16 motifs (Fig. 3C).

Analysis of cis-acting elements in *PutGRXs* promoters

To investigate the potential functions of *PutGRXs*, a prediction of cis-acting elements was made in 25 *PutGRX* promoter regions and a schematic map was created of the prevalent distributions of stress and hormone responsive *cis*-acting elements (Fig. 4A). A total of 988 cis-acting elements in *PutGRXs* were predicted, which were associated with various abiotic stresses, including light (194 elements), drought (312), heat (108), anaerobic conditions (60), wounding (25), cold (18), and phytohormones (270) (Fig. 4B and Supplemental Table S6). Among these,

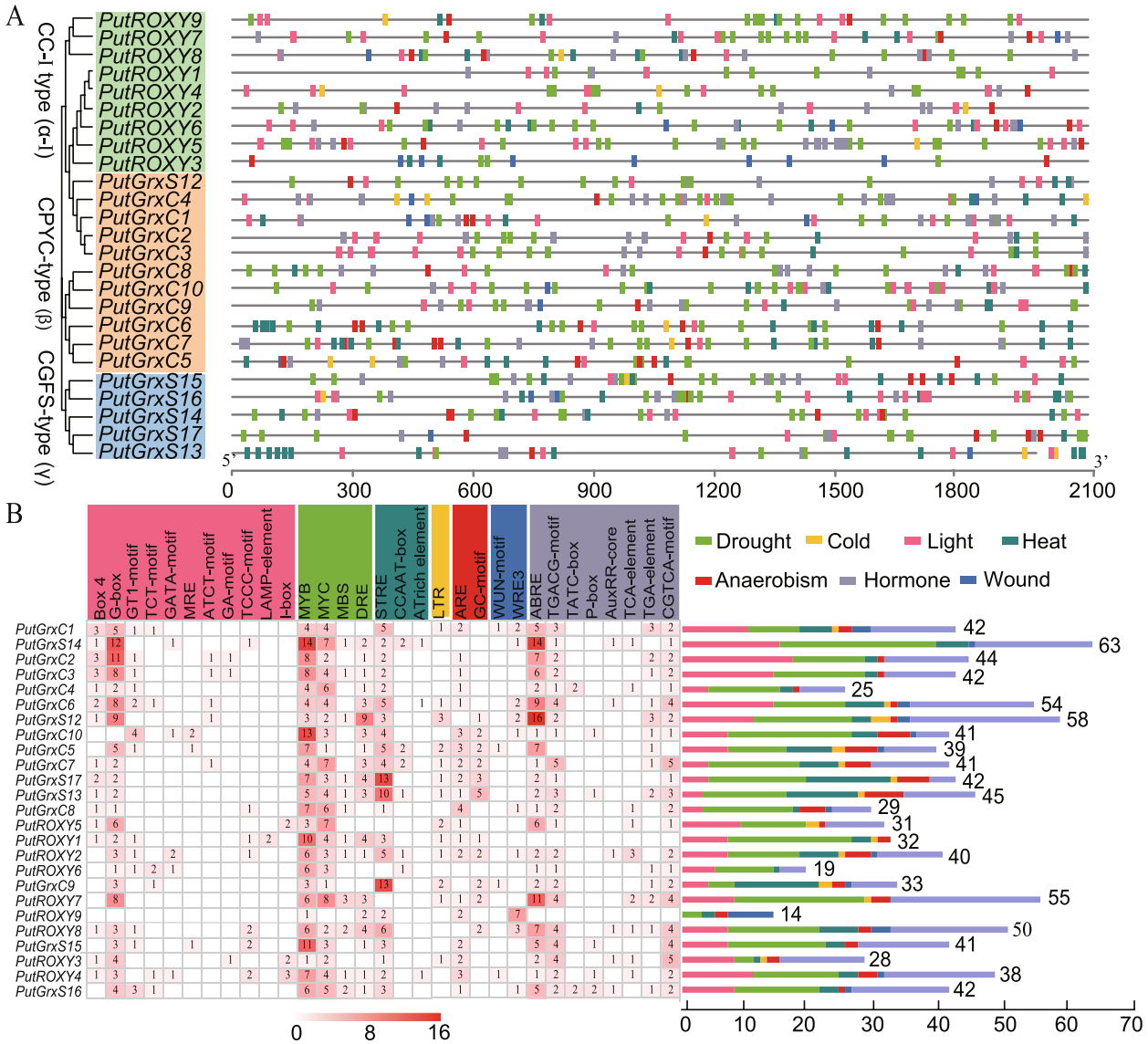

Fig. 4 Analysis of cis-acting elements in the promoter region of the *PutGRXs* gene. **A** The *cis*-acting elements distribution in *PutGRX* promoter regions. **B** The names and numbers of *cis*-acting elements in *PutGRX* promoters. The heatmap in grid and the color columns indicated the numbers of *cis*-acting elements. ABRE: ABA responsive element, ARE: Anaerobic- responsive element, DRE: Dehydration- responsive element, JERE: Jasmonate and/or elicitor responsive element, LTR: Low temperature- responsive element, MBS: MYB-binding site, MRE: Metal response element, MRS: MYB recognition site, MYB: v-myb avian myeloblastosis viral oncogene homolog, MYC: Myelocytomatosis; WRE3: Wound response element 3

certain elements responsive to drought (e.g., DRE, MYB, MRS, MYC, and MBS), light-responsive elements (e.g., DRE, MYB, MRS, MYC, and MBS), and heat-responsive elements (e.g., CCAAT-box, STRE, and AT-rich), and phytohormones together account for a significant portion of the total in each of the *PutGRX*, some of which are conserved among the 25 *PutGRXs* (Fig. 4B). These findings suggest that *PutGRXs* play vital roles in responding to drought, light, heat, and hormonal signals. It is noteworthy that a total of 312 drought-responsive elements were identified, containing 154 MYBs, 95 MYCs, 16 MBSs, and 48 DREs. Additionally, 270 hormone-responsive elements were detected, including 115 ABA (also known as ABRE), 106 methyl jasmonate (MeJA) (specifically TGACG and CGTCA motifs), and 12 salicylic acid (SA) (identified as TCA element), 18 gibberellin (GA) (specifically P-box and TATC-box), and 27 auxin (specifically TGA-element and AuxRR-core) (Fig. 4B). The conserved elements found in the promoter region indicate

that *PutGRXs* plays a crucial role in responding to abiotic stresses and phytohormone treatments.

Predicted subcellular localization of PutGRXs

To predict the subcellular localization of PutGRXs, all 25 protein sequences of PutGRXs were submitted to four internet tools (Fig. 5A, Supplemental Table S7). The results of the prediction indicated that all of the nine CC-type GRXs (PutROXY1 to PutROXY9) were cytoplasm-localized, and two of them were also localized in the nucleus (PutROXY2) or the plastids/chloroplasts (PutROXY3) (Fig. 5A). In addition, all of the 11 CPYC-type GRXs and four CGFS-type GRXs were localized in the plastids/chloroplasts, while a CGFS-type PutGrxS15 was specially localized in the mitochondrion. Among them, five PutGRXs (i.e. PutGrxC2, PutGrxC5, PutGrxC6, PutGrxC8, PutGrxS16) were simultaneously localized in the plastids/chloroplasts, while PutGrxC6 and PutGrxC8 were also localized in the nucleus or cytoplasm (Fig. 5A). Furthermore, PutGrxC7, PutGrxS14, PutGrxS13 and PutGrxS17 were localized in the cytoplasm or nucleus in addition to the plastids/chloroplasts localization (Fig. 5A).

Tissue and organ specific expression analysis of *PutGRXs*

To obtain a more profound comprehension of the specific expression of the 25 *PutGrx* genes, an extraction of the complete RNA was conducted from the roots, leaves, stems, flowers, and sheaths of alkaligrass. The transcript levels of *PutGrx* genes were evaluated using RT-qPCR analysis (Fig. 5A, Supplemental Table S8). When compared with roots, the CC-type *PutROXY2*, five CPYC-type *GRXs* (*PutGrxC1*, *PutGrxC2*, *PutGrxC3*, *PutGrxC5*, and *PutGrxC6*), and two CGFS-type *GRXs* (*PutGrxS14* and *PutGrxS15*) were highly expressed in all the other tissues and organs (i.e., leaves, stems, flowers, and sheaths) (Fig. 5A). Furthermore, the relative expressions of *PutGrxS12* and *PutROXY5* were higher in stems, flowers, and sheaths, while *PutROXY6*, *PutGrxC8*, and *PutGrxC9* were enriched in flowers and sheaths (Fig. 5A). Conversely, *PutGrxC10* and *PutGrxC7* exhibited lower levels in all other tissues and organs when compared with those in roots (Fig. 5A). This finding indicates that these PutGRXs may possess distinct biological functions in diverse tissues and organs.

Salinity response of the representative *PutGRXs* in leaves and roots

To investigate the salt response patterns of *PutGRXs*, three-week-old alkaligrass seedlings were treated with 100 mM NaCl, 100 mM $NaHCO_3$, and 50 mM Na_2CO_3 for 24 h, respectively. Twelve *PutGRXs* that had been successfully cloned by us were selected as representative genes. These expression levels of these genes were then evaluated using RT-qPCR analysis (Fig. 5B and C, Supplemental Table S9 and S10).

In leaves, *PutGrxS12* and *PutGrxC1* were significantly induced under all salt stress conditions, while *PutGrxC3* and *PutGrxC4* were increased under NaCl and $NaHCO_3$ treatments. Conversely, *PutGrxC5* was obviously upregulated under Na_2CO_3 conditions, yet downregulated under NaCl and $NaHCO_3$ treatments. *PutGrxC9* and *PutROXY9* were induced under $NaHCO_3$ but reduced under NaCl and/or Na_2CO_3 stresses. In contrast, the other four PutGRXs (*PutGrxC2*, *PutGrxC6*, *PutROXY7*, and *PutROXY5*) demonstrated a significant reduction in response to all salt stress conditions (Fig. 5B).

In roots, five CPYC-type *GRXs* (*PutGrxC9*, *PutGrxC6*, *PutGrxC2*, *PutGrxC5*, and *PutGrxC3*) and three CC-type *GRXs* (*PutROXY7*, *PutROXY9*, and *PutROXY5*) were induced, while three *PutGRXs* (*PutGrxS12*, *PutGrxC1*, and *PutROXY8*) were reduced under NaCl treatment (Fig. 5C). Furthermore, only three *PutGRXs* (*PutGrxC9*, *PutGrxC6*, and *PutROXY7*) were upregulated under $NaHCO_3$ treatment, and three *PutGRXs* (*PutGrxC9*, *PutGrxC4*, and *PutROXY9*) were increased under Na_2CO_3

(See figure on next page.)

Fig. 5 Tissue- and organ- specific expression, salt- and alkali- responsive expression, protein structure, and subcellular localization of PutGRXs. **A** Tissue- and organ- specific expression *PutGRXs* were analyzed in roots, leaves, stems, flowers, and sheaths using RT-qPCR analysis. C: cytoplasm, M: mitochondrion, N: nucleus, P: plastid. **B** Salt- and alkali- responsive expression pattern in leaves of PutGRXs. **C** Salt- and alkali- responsive expression pattern in roots of *PutGRXs*. The data represented the expression levels of *PutGRXs* after treatments of 50 mmol L^{-1} Na_2CO_3, 100 mmol L^{-1} NaCl, and 100 mmol L^{-1} $NaHCO_3$ (pH 9.0) for 24 h, respectively. The RT-qPCR results were calculated via the $2^{-\Delta\Delta Ct}$ method, and the reference gene (*PutActin*) was used to correct the expression levels of *PutGRXs*. The heatmap of *PutGRXs* expression based on the RT-qPCR data standardized by log2 conversion. The color bar on the right of the heat map was based on the RT-qPCR data. Red and blue colors indicated up- and down- regulated genes, respectively. **D** Sequence comparison of amino acids of GrxS12 of *Puccinellia tenuiflora*, and its homologues from *Oryza sativa*, *Arabidopsis thaliana*, and *Populus trichocarpa*. The atypical CPYC-motif and the conserved cysteines were marked. **E** Predicted protein 3D structure of PutGrxS12. The cysteine 136 and cysteine 78 were marked. The AlphaFold database was utilized to predict the 3D structure of the PutGRX protein. The predicted 3D structures of proteins were visualized using Pymol software. **F** Subcellular localization of PutGrxS12 and its three cysteine mutations ($PutGrxS12^{C78S}$, $PutGrxS12^{C136S}$ and $PutGrxS12^{C78S/C136S}$) in Arabidopsis protoplasm cells. 35S::GFP indicated the vector control. All proteins were transiently expressed in protoplasm cells from Arabidopsis leaves, and the GFP signal was visualized after 12 h. Bar = 40 μm

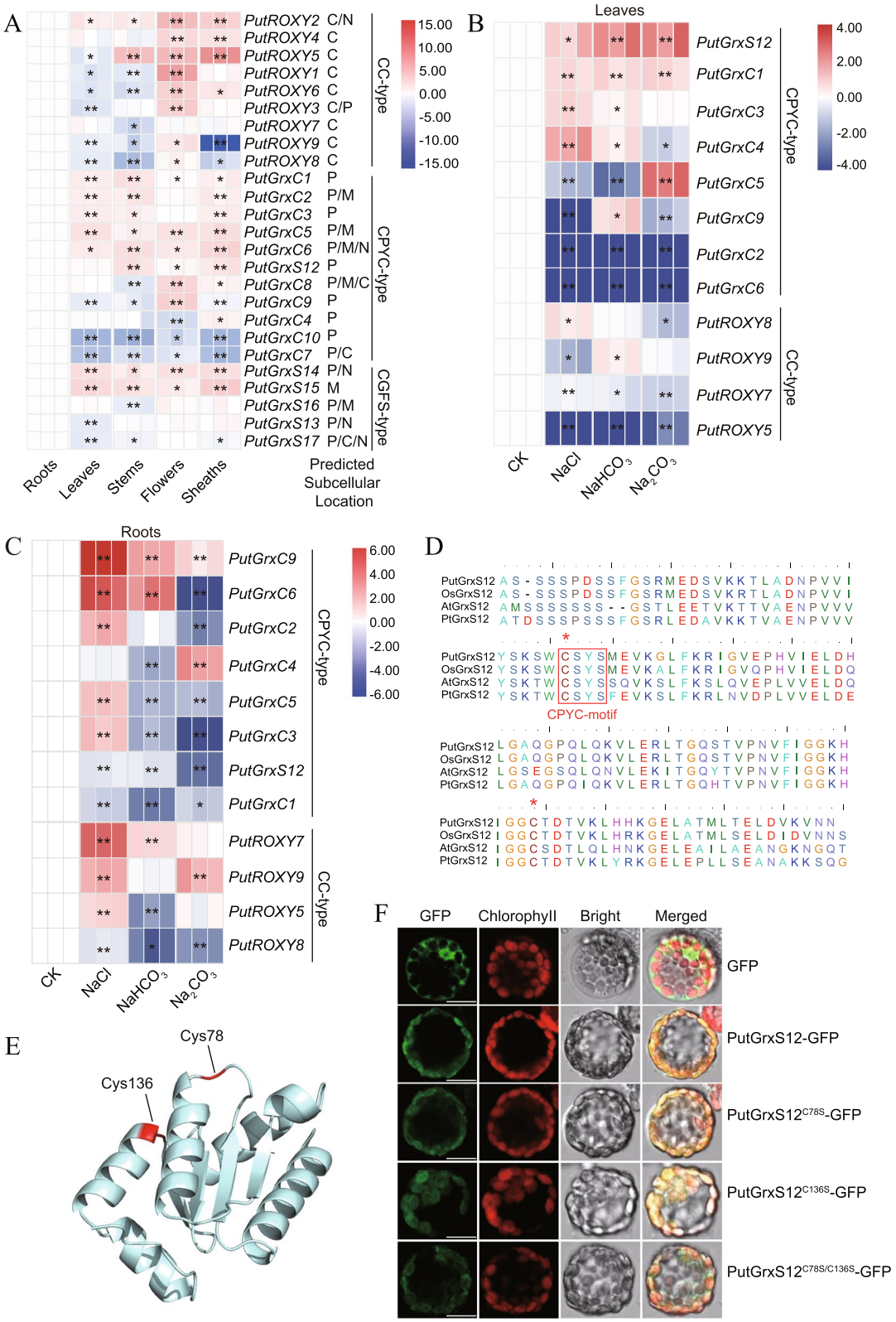

Fig. 5 (See legend on previous page.)

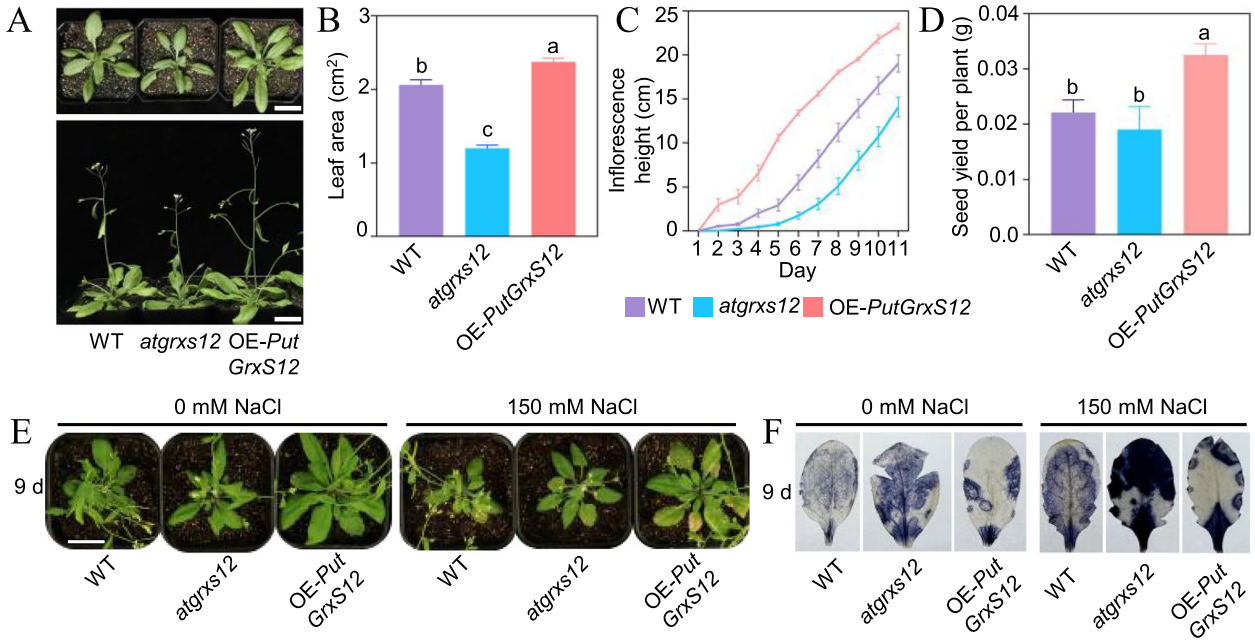

Fig. 6 The growth and salt-responsive phenotypes of wild-type, *atgrxs12* mutant and *PutGrxS12*-overexpressing Arabidopsis plants. **A** The growth phenotypes of four-week-old wild-type, *atgrxs12* mutant and *PutGrxS12*-overexpressing Arabidopsis plants. **B**, **C** Leaf area of the 7 th and 8 th leaves and inflorescence length of seedlings in (**A**). **D** Seed yield per plant of wild-type, *grxs12* mutant and *PutGrxS12*-overexpressing Arabidopsis. **E** Salt-responsive phenotypes of wild-type, *atgrxs12* mutant and *PutGrxS12*-overexpressing Arabidopsis plants. Four-week seedlings were treated with 150 mM NaCl for nine days. **F** The accumulation of $O_2^{\cdot-}$ in the leaves. The $O_2^{\cdot-}$ levels of leaves from wild-type, *atgrxs12* mutant and *PutGrxS12*-overexpressing Arabidopsis plants under 0 mM and 150 mM NaCl treatment were detected using NBT staining method

treatment, while the majority of the remaining *PutGRXs* were reduced under $NaHCO_3$ and Na_2CO_3 treatments (Fig. 5C).

Protein structure and subcellular localization of PutGrxS12

The PutGrxS12 was significantly induced in leaves, but reduced in roots under various salt conditions. To further investigate the biological function of PutGrxS12, a multiple sequence alignment analysis was conducted among the following: alkaligrass PutGrxS12 and its three homogenous forms from Arabidopsis, rice, and poplar. The amino acid sequence of PutGrxS12 exhibited similarities with other GrxS12s, featuring a conserved atypical CPYC motif and a secondary cysteine in the C-terminal region (Fig. 5D).

The 3D structure of PutGrxS12 was predicted using the AlphaFold protein structure database (https://alphafold.ebi.ac.uk/). The 3D structure exhibited that PutGrxS12 contains five α-helixes and four β-folds (Fig. 5E). The Fig. 5E illustrates the location of two conserved cysteines (Cys78 and Cys136) (Fig. 5E). In GRX, the functional motif cysteine and C-terminal cysteine were demonstrated to function synergistically in regulating enzymatic activity [39].

The subcellular localization of PutGrxS12 was performed using Arabidopsis protoplasts. The genetic fusion of PutGrxS12 and its cysteine site mutations ($PutGrxS12^{C78S}$, $PutGrxS12^{C136S}$, and $PutGrxS12^{C78S/C136S}$) was achieved by fusing them in frame to the 3'-terminus of the GFP reporter gene, with the CaMV 35S promoter serving as the regulatory element. The transient expression of the recombinant PutGrxS12-GFP, its three mutant variations, and the GFP in protoplast cells revealed that the 35S::GFP signal was visible throughout the cytoplasm, nucleus, and plasma membrane, whereas the PutGrxS12-GFP signal was concentrated in the chloroplasts (Fig. 5F). This finding indicates that the recombinant PutGrxS12-GFP protein is localized in chloroplasts/plastids and that the cysteine mutations do not affect its subcellular localization.

PutGrxS12 is essential for plant growth and ROS scavenging

To investigate the biological function of PutGrxS12, we constructed transgenic Arabidopsis plants overexpressing *PutGrxS12* under the control of the CaMV35S promoter. Four-week-old seedlings of Arabidopsis wild type (WT), *atgrxs12* mutant, and *PutGrxS12* overexpressing (OE-*PutGrxS12*) seedlings were utilized to analyze the growth and salt stress phenotypes (Fig. 6). The four-week-old seedlings of the *atgrxs12* mutant plants exhibited slow growth, reduced plant height, decreased rosette

leaf area, and diminished seed production. Conversely, the OE-*PutGrxS12* seedlings showed accelerated growth, an enlarged rosette leaf area, elevated plant height, and increased seed production in comparison to the WT plants (Fig. 6A-D). This finding suggests that PutGrxS12 is essential for plant growth.

When the WT, *atgrxs12* mutant, and OE-*PutGrxS12* seedlings were treated with 150 mM NaCl for nine days, all the salinity-treated plants showed slow growth and the leaves exhibited signs of wilting and yellowing, accompanied by water loss (Fig. 6E). The accumulation of $O_2^{\cdot-}$ in the leaves of various Arabidopsis seedlings was visualized by NBT staining. The $O_2^{\cdot-}$ level was induced in *atgrxs12* mutant seedlings, but reduced in the OE-*PutGrxS12* seedlings in comparison to the WT plants under normal conditions. Following NaCl treatment, $O_2^{\cdot-}$ levels were increased in all seedlings, while the *atgrxs12* mutant showed a significant amount of ROS accumulation (Fig. 6F). This indicates that PutGrxS12 is critical for ROS scavenging, especially in salt stress conditions.

Discussion

Classification and nomenclature standardization of plant GRX gene families

GRXs are small, ubiquitous oxidoreductases belonging to the thioredoxin superfamily. These enzymes, dependent on either glutathione (GSH) or thioredoxin reductase (TR) for their activity, are present in most eukaryotic and prokaryotic organisms, with the exception of certain bacterial and archaeal species [40]. Phylogenetic analyses reveal that the GRX gene family represents a highly complex and diversified group that has undergone significant expansion throughout evolution. This expansion has resulted in variations in GRX classes and gene content across plant species at different evolutionary stages—from algae, mosses, and ferns to gymnosperms and angiosperms [26]. For instance, the model species *Arabidopsis thaliana* and rice possess 31 and 29 *GRX* genes in their respective genomes [26].

The continuous sequencing of plant genomes and discovery of new *GRXs* has led to ongoing evolution in the classification and nomenclature of *GRX* gene family members. Analysis of 58 genomes from prokaryotic and eukaryotic photosynthetic organisms has established six GRX classes (I-VI), with only classes I and II demonstrating evolutionary conservation across all photosynthetic species [26]. Despite this classification system, significant inconsistencies persist in plant GRX nomenclature across studies. Current challenges include the lack of standardized naming conventions for subclasses [26] and multiple designations for identical GRX proteins [37, 41], potentially leading to misinterpretation in comparative analyses. To address these nomenclature issues, Xu et al. [34] conducted a comprehensive evolutionary study of 14 gene families across land plants (spanning bryophytes to angiosperms), classifying 412 *GRX* genes into four well-defined clades: Alpha (CC-type), Beta (CPYC-type), Gamma (CGFS-type), and Delta (novel group). Their systematic approach incorporated multiple molecular characteristics, including gene architecture, expression profiles, subcellular distribution, catalytic properties, and substrate recognition [34]. Applying this framework to *Populus trichocarpa*, Xu et al. identified and categorized 41 *GRX* genes [34]. In our current investigation of alkaligrass, we have classified 25 putative PutGRXs into three major groups based on amino acid sequence features: CC-type (alpha clade), CPYC-type (beta clade), and CGFS-type (gamma clade) (Fig. 3A). This classification aligns with Xu et al.'s nomenclature system, enabling more accurate cross-species comparisons while resolving previous terminological inconsistencies.

Evolutionary divergence and functional adaptation of GRX families

GRXs constitute a crucial component of plant redox systems, playing pivotal roles in stress responses and developmental processes. In addition to halophyte alkaligrass (*Puccinellia tenuiflora*), GRX gene families have been characterized in seven other plant species: herbaceous model *Arabidopsis thaliana* [16], monocot crop rice (*Oryza sativa*) [37], maize (*Zea mays*) [42], woody perennial poplar (*Populus trichocarpa*) [34], allotetraploid crop cotton (*Gossypium hirsutum*) [43], clonally propagated fruit banana (*Musa acuminata*) [44], and legume common bean (*Phaseolus vulgaris*) [45].

The evolutionary trajectory of *GRX* genes has been profoundly shaped by various duplication events across plant species, with distinct patterns emerging in different lineages. Poplar exhibits the most pronounced duplication rate among the studied species, with approximately 32% (13/41) of its *GRX* genes resulting from duplication events [34]. Cotton displays specialized subgenome-specific retention patterns reflective of its allotetraploid nature [43]. Both rice and alkaligrass have developed stress-associated tandem arrays, suggesting adaptive evolution in response to environmental pressures [37]. Banana stands out with its unique lineage-specific expansions [44], while common bean demonstrates legume-specific duplication events that may be linked to its symbiotic nitrogen-fixing capabilities [45]. These diverse duplication patterns collectively highlight how different evolutionary pressures and life history traits have driven the expansion and diversification of *GRX* gene families through whole-genome and tandem duplication events in various plant lineages.

The *GRX* gene family comprises three evolutionarily conserved subgroups that exhibit both conserved features and species-specific structural variations. Subgroup I, characterized by CPYC/CGYC/CPFC/CSYC motifs, typically contains 4–5 exons across most species, though cotton displays elongated N-terminal regions in certain isoforms [43], while alkaligrass has evolved unique CP[K/R]C variants. Subgroup II (CGFS) shows more complex domain architectures, with banana and cotton possessing multi-domain structures [43, 44], contrasting with common bean truncated forms that lack characteristic C-terminal motifs [45]. The CC-type Subgroup III is predominantly composed of single-exon genes, except in cotton, with alkaligrass containing novel CCMC variants and banana exhibiting distinctive fusion proteins incorporating F-box domains [44]. These structural variations reflect both the conserved redox functions and lineage-specific adaptations of GRX proteins across plant species.

Bioinformatic analysis of promoter regions has identified both conserved and species-specific *cis*-regulatory elements governing *GRX* gene expression in these plant species. They maintain core stress-responsive elements (ABRE, MYB, and W-box) in *GRX* promoters, indicating evolutionary conservation of stress regulation mechanisms. Notably, alkaligrass shows significant enrichment of salt-responsive elements (MYB and NAC), consistent with its halophytic adaptation. Cotton possesses unique fiber development-associated motifs, reflecting its specialized role in cotton fiber formation [43]. Banana contains fruit ripening-related regulatory elements that correlate with its edible fruit characteristics [44], while common bean exhibits nodulation-specific motifs, likely associated with its symbiotic nitrogen-fixing capacity [45]. These distinct *cis*-element profiles demonstrate how *GRX* genes have acquired lineage-specific regulatory features while maintaining core stress-response functions across plant species.

The *GRX* gene family exhibits extraordinary evolutionary adaptability across plant lineages, with distinct functional specializations emerging in different ecological contexts. In woody species like poplar, gene family expansion has preferentially maintained chloroplast-targeted GRX isoforms, likely supporting the enhanced photosynthetic demands of perennial growth [34]. Domesticated crops such as rice and cotton display characteristic specialization patterns that reflect human selection pressures during crop improvement [37, 43]. Remarkably, extremophyte species including alkaligrass have evolved stress-optimized GRX variants with enhanced protective functions, while fruit-bearing plants like banana have developed sophisticated ripening-related regulatory networks involving GRX-mediated redox control [44]. These demonstrate how the fundamental redox functions of GRX proteins have been exquisitely tailored to meet the specific physiological demands of different plant life strategies and ecological niches.

Functional differentiation of CC-type and CPYC-type PutGRXs in salinity response

It has been demonstrated that CC-type GRXs play a regulatory role in floral organ development (e.g., anthers and petals) and pathogen defense [46]. In alkaligrass, eight of the nine CC-type PutGRXs were highly expressed in flowers, with four showing enrichment in sheaths (Fig. 5A). This finding aligns with previous reports on CC-type GRXs in Arabidopsis and rice [46]. In contrast, CPYC-type GRXs are known to play a significant role in oxidative stress responses [47]. Salinity stress induces ROS accumulation in plants, disrupting cellular redox homeostasis [48]. Our results revealed four CPYC-type *PutGRXs* were induced in leaves by NaCl and $NaHCO_3$, while two responded to Na_2CO_3. In roots, five were induced by NaCl, two by $NaHCO_3$, and one by Na_2CO_3 (Fig. 5B, C). Notably, three CC-type *GRXs* were significantly upregulated in roots under NaCl stress, with two also responding to $NaHCO_3$ or Na_2CO_3 (Fig. 5C). This suggests that GRXs in alkaligrass play a broader role in salinity-induced oxidative stress responses compared to Arabidopsis [47]. Unlike CC- and CPYC-type GRXs, CGFS-type GRXs are primarily involved in [Fe-S] cluster assembly [49]. However, we did not clone CGFS-type PutGRXs in this study, leaving their functional characterization in alkaligrass for future investigation. Additionally, molecular genetic studies have shown that GRXs from various plant species enhance salt tolerance. For example, overexpression of tomato *SlGrx1* [50], rice *OsGrx8* [51], and chickpea *CaGrx* [52] in *Arabidopsis* improved salt tolerance. Similarly, overexpression of rice *OsGrx20* and *OsGrxC7* enhanced salt tolerance in rice [53, 54]. Despite these advances, the detailed regulatory mechanisms remain unclear, warranting further research.

Chloroplast GRXs are essential for plant growth and stress response

Plant chloroplasts serve as crucial photosynthetic organelles and primary sites for synthesizing numerous secondary metabolites. During these metabolic processes, excess reactive oxygen species (ROS) can oxidize nucleic acids, proteins, lipids and other cellular components, disrupting redox homeostasis and metabolic balance. Chloroplast GRXs play an important role in maintaining protein redox states and regulating chloroplast metabolic equilibrium [55–59]. Our results predicted that 16 PutGRXs in alkaligrass likely localize to chloroplasts, with most responding to salinity stresses (Fig. 5A-C). Genetics analysis indicated that chloroplast-localized PutGrxS12

was essential for alkaligrass growth and ROS scavenging (Fig. 6). Arabidopsis chloroplasts contain four GRXs: AtGrxS14, AtGrxS16, AtGrxS12 and AtGrxC5 [13, 26, 28, 39, 47, 60]. Among these, AtGrxS14 and AtGrxS16 showed widespread expression across Arabidopsis organs, with particularly high abundance in photosynthetic tissues like young leaves compared to roots and flowers [61]. While single *atgrxs14* or *atgrxs16* mutant displayed no obvious phenotypes under normal conditions, double mutants exhibit significantly reduced rosette weight [61] The chlorophyll contents decreases in plants lacking *AtGrxS14*, while overexpressing either *AtGrxS14* or *AtGrxS16* reduced the abundances of NifU-like protein 2 (NFU2) and SulfurE 1 (SufE1)—two key proteins involved in Fe-S protein maturation [61]. These findings suggest functional redundancy between *AtGrxS14* and *AtGrxS16* in regulating Fe-S cluster transfer. Notably, AtGrxS16 possesses a unique domain architecture, combining an N-terminal endonuclease domain with a C-terminal GRX domain, potentially linking redox regulation with chloroplast DNA metabolism [60].

Chloroplast GRXs participate in diverse stress response pathways. Under high-light conditions, both AtGrxS14 and AtGrxS16 protein levels decrease [61]. However, AtGrxS14 shows increased expression in response to low temperature, salt, and drought stresses [61]. Functional studies demonstrate that overexpression of *AtGrxS14*—but not *AtGrxS16*—enhances plant growth under high-light, low temperature, and drought conditions [61].

Both *AtGrxS14* and *AtGrxS16* interacted with selenium-binding protein (SBP) to mediate selenium stress tolerance [62]. Supporting their stress-related functions, tomato plants with silenced *SlGRXS16* expression exhibit increased sensitivity to osmotic stress [50]. Interestingly, knockout of *GrxC5* in the moss *Physcomitrium patens* shows no detectable growth defects or stress sensitivity, with protein cysteine disulfide formation rates and S-glutathionylation levels remaining unchanged following H_2O_2 treatment [63]. Our findings indicate that chloroplast-localized PutGRXs contribute to salinity stress tolerance regulation in alkaligrass. However, the specific molecular mechanisms governing these PutGRX-mediated responses require further investigation.

Conclusions

Alkaligrass (*P. tenuiflora*) is a highly salt-tolerant forage species whose evolutionary adaptation to saline environments may be partially attributed to gene family expansion [2]. As crucial oxidoreductases, plant GRXs play vital roles in developmental regulation and stress responses. In this study, we characterized the *GRX* gene family in alkaligrass, identifying 25 PutGRXs classified into three types: CGFS-type, CPYC-type and CC-type. Promoter analyses revealed that these PutGRXs likely participate in diverse stress response pathways. Through RT-qPCR validation, we demonstrated that most PutGRXs respond to various saline-alkaline stress conditions. Molecular genetics experiments further revealed that PutGrxS12 plays a critical role in maintaining plant growth and ROS homeostasis. Our findings provide important insights into the redox regulatory mechanisms mediated by PutGRXs in alkaligrass. However, the specific protein targets regulated by GRXs and the molecular mechanisms underlying GRX-mediated redox regulation of substrate proteins require further investigation.

Supplementary Information

The online version contains supplementary material available at https://doi.org/10.1186/s12870-025-06547-1.

Supplementary Material 1.

Authors' contributions

S.D. and Y.L. designed and supervised the study; Y.L., X.H., J.Y., Y.L. M.S. and Q.P. analyzed the data and visualized the results; Y.L., S.D. and Y.L. wrote the initial manuscript; All other authors contributed critically to the writing of the final manuscript and gave approval for publication.

Funding

This work was supported by the National Natural Science Foundation of China (No. 32441006 and 32070300); and the Fund of Shanghai Engineering Research Center of Plant Germplasm Resources, China (No. 17DZ2252700) to Shaojun Dai, the Open Fund of Key Laboratory of Saline-alkali Vegetation Ecology Restoration (Northeast Forestry University), Ministry of Education (No. 0924210102) and the Natural Science Foundation of Shanghai (No. 22ZR1445700) to Meihong Sun, and the Spring Wild Goose Support Program for Outstanding Young Sci-Tech Talents in Heilongjiang Province (CYQN24057) to Qiuying Pang.

Data availability

Data is provided within the manuscript or supplementary information files.

Declarations

Ethics approval and consent to participate

Not applicable.

Consent for publication

Not applicable.

Competing interests

The authors declare no competing interests.

Received: 2 March 2025 Accepted: 11 April 2025
Published online: 08 May 2025

References

1. Zhang X, Wei L, Wang Z, Wang T. Physiological and molecular features of *Puccinellia tenuiflora* tolerating salt and alkaline-salt stress. J Integr Plant Biol. 2013;55(3):262–76.
2. Zhang W, Liu J, Zhang Y, Qiu J, Li Y, Zheng B, Hu F, Dai S, Huang X. A high-quality genome sequence of alkaligrass provides insights into halophyte stress tolerance. Sci China Life Sci. 2020;63(9):1269–82.

3. Yu J, Chen S, Zhao Q, Wang T, Yang C, Diaz C, Sun G, Dai S. Physiological and proteomic analysis of salinity tolerance in *Puccinellia tenuiflora*. J Proteome Res. 2011;10(9):3852–70.
4. Yu J, Chen S, Wang T, Sun G, Dai S. Comparative proteomic analysis of *Puccinellia tenuiflora* leaves under Na_2CO_3 stress. Int J Mol Sci. 2013;14(1):1740–62.
5. Zhao Q, Suo J, Chen S, Jin Y, Ma X, Yin Z, Zhang Y, Wang T, Luo J, Jin W, et al. Na_2CO_3-responsive mechanisms in halophyte *Puccinellia tenuiflora* roots revealed by physiological and proteomic analyses. Sci Rep. 2016;6:32717.
6. Meng X, Zhao Q, Jin Y, Yu J, Yin Z, Chen S, Dai S. Chilling-responsive mechanisms in halophyte *Puccinellia tenuiflora* seedlings revealed from proteomics analysis. J Proteomics. 2016;143:365–81.
7. Yu J, Zhang Y, Liu J, Wang L, Liu P, Yin Z, Guo S, Ma J, Lu Z, Wang T, et al. Proteomic discovery of H_2O_2 response in roots and functional characterization of *PutGLP* gene from alkaligrass. Planta. 2018;248(5):1079–99.
8. Yin Z, Zhang H, Zhao Q, Yoo M-J, Zhu N, Yu J, Yu J, Guo S, Miao Y, Chen S, et al. Physiological and comparative proteomic analyses of saline-alkali $NaHCO_3$-responses in leaves of halophyte *Puccinellia tenuiflora*. Plant Soil. 2019;437:137–58.
9. Zhang Y, Zhang Y, Yu J, Zhang H, Wang L, Wang S, Guo S, Miao Y, Chen S, Li Y, et al. NaCl-responsive ROS scavenging and energy supply in alkaligrass callus revealed from proteomic analysis. BMC Genomics. 2019;20(1):990.
10. Suo J, Zhang H, Zhao Q, Zhang N, Zhang Y, Li Y, Song B, Yu J, Cao J, Wang T, et al. Na_2CO_3-responsive photosynthetic and ROS scavenging mechanisms in chloroplasts of alkaligrass revealed by phosphoproteomics. Genomics Proteomics Bioinformatics. 2020;18(3):271–88.
11. Zhang H, Han B, Wang T, Chen S, Li H, Zhang Y, Dai S. Mechanisms of plant salt response: insights from proteomics. J Proteome Res. 2012;11(1):49–67.
12. Yu J, Li Y, Qin Z, Guo S, Li Y, Miao Y, Song C, Chen S, Dai S. Plant chloroplast stress response: insights from thiol redox proteomics. Antioxid Redox Signal. 2020;33(1):35–57.
13. Couturier J, Ströher E, Albetel A-N, Roret T, Muthuramalingam M, Tarrago L, Seidel T, Tsan P, Jacquot J-P, Johnson MK, et al. Arabidopsis chloroplastic glutaredoxin C5 as a model to explore molecular determinants for iron-sulfur cluster binding into glutaredoxins. J Biol Chem. 2011;286(31):27515–27.
14. Inigo S, Nagels Durand A, Ritter A, Le Gall S, Termathe M, Klassen R, Tohge T, De Coninck B, Van Leene J, De Clercq R, et al. Glutaredoxin GRXS17 associates with the cytosolic iron-sulfur cluster assembly pathway. Plant Physiol. 2016;172(2):858–73.
15. Gutsche N, Holtmannspötter M, Maß L, O'Donoghue M, Busch A, Lauri A, Schubert V, Zachgo S. Conserved redox-dependent DNA binding of ROXY glutaredoxins with TGA transcription factors. Plant Direct. 2017;1(6):e00030.
16. Rouhier N, Couturier J, Jacquot JP. Genome-wide analysis of plant glutaredoxin systems. J Exp Bot. 2006;57(8):1685–96.
17. Karplus PA, Schulz GE. Substrate binding and catalysis by glutathione reductase as derived from refined enzyme: substrate crystal structures at 2 A resolution. J Mol Biol. 1989;210(1):163–80.
18. Lemaire SD, Miginiac-Maslow M. The thioredoxin superfamily in *Chlamydomonas reinhardtii*. Photosynth Res. 2004;82(3):203–20.
19. Trnka D, Engelke AD, Gellert M, Moseler A, Hossain MF, Lindenberg TT, Pedroletti L, Odermatt B, de Souza JV, Bronowska AK, et al. Molecular basis for the distinct functions of redox-active and FeS-transfering glutaredoxins. Nat Commun. 2020;11(1):3445.
20. Roret T, Tsan P, Couturier J, Zhang B, Johnson MK, Rouhier N, Didierjean C. Structural and spectroscopic insights into BolA-glutaredoxin complexes. J Biol Chem. 2014;289(35):24588–98.
21. Moseler A, Aller I, Wagner S, Nietzel T, Przybyla-Toscano J, Mühlenhoff U, Lill R, Berndt C, Rouhier N, Schwarzländer M, et al. The mitochondrial monothiol glutaredoxin S15 is essential for iron-sulfur protein maturation in *Arabidopsis thaliana*. Proc Natl Acad Sci U S A. 2015;112(44):13735–40.
22. Martins L, Knuesting J, Bariat L, Dard A, Freibert SA, Marchand CH, Young D, Dung NHT, Voth W, Debures A, et al. Redox modification of the iron-sulfur glutaredoxin grxs17 activates holdase activity and protects plants from heat stress. Plant Physiol. 2020;184(2):676–92.
23. Elgán Tobias H, Planson A-G, Beckwith J, Güntert P, Berndt KD. Determinants of activity in glutaredoxins: anin vitroevolved Grx1-like variant of *Escherichia coli* Grx3. Biochem J. 2010;430(3):487–95.
24. Yu J, Zhang NN, Yin PD, Cui PX, Zhou CZ. Glutathionylation-triggered conformational changes of glutaredoxin Grx1 from the yeast *Saccharomyces cerevisiae*. Proteins. 2008;72(3):1077–83.
25. Liu X, Jann J, Xavier C, Wu H. Glutaredoxin 1 (Grx1) protects human retinal pigment epithelial cells from oxidative damage by preventing AKT glutathionylation. Invest Ophthalmol Vis Sci. 2015;56(5):2821–32.
26. Couturier J, Jacquot JP, Rouhier N. Evolution and diversity of glutaredoxins in photosynthetic organisms. Cell Mol Life Sci. 2009;66(15):2539–57.
27. Tarrago L, Laugier E, Zaffagnini M, Marchand C, Le Maréchal P, Rouhier N, Lemaire SD, Rey P. Regeneration mechanisms of *Arabidopsis thaliana* methionine sulfoxide reductases B by glutaredoxins and thioredoxins. J Biol Chem. 2009;284(28):18963–71.
28. Zaffagnini M, Bedhomme M, Marchand CH, Couturier J, Gao X-H, Rouhier N, Trost P, Lemaire SD. Glutaredoxin S12: unique properties for redox signaling. Antioxid Redox Signal. 2012;16(1):17–32.
29. Xiang C, Werner BL, Christensen EM, Oliver DJ. The biological functions of glutathione revisited in arabidopsis transgenic plants with altered glutathione levels. Plant Physiol. 2001;126(2):564–74.
30. Huang LJ, Li N, Thurow C, Wirtz M, Hell R, Gatz C. Ectopically expressed glutaredoxin ROXY19 negatively regulates the detoxification pathway in *Arabidopsis thaliana*. BMC Plant Biol. 2016;16(1):200.
31. Ndamukong I, Abdallat AA, Thurow C, Fode B, Zander M, Weigel R, Gatz C. SA-inducible Arabidopsis glutaredoxin interacts with TGA factors and suppresses JA-responsive PDF1.2 transcription. Plant J. 2007;50(1):128–39.
32. Zander M, Chen S, Imkampe J, Thurow C, Gatz C. Repression of the *Arabidopsis thaliana* jasmonic acid/ethylene-induced defense pathway by TGA-interacting glutaredoxins depends on their C-terminal ALWL motif. Mol Plant. 2012;5(4):831–40.
33. Uhrig JF, Huang LJ, Barghahn S, Willmer M, Thurow C, Gatz C. CC-type glutaredoxins recruit the transcriptional co-repressor TOPLESS to TGA-dependent target promoters in *Arabidopsis thaliana*. Biochim Biophys Acta Gene Regul Mech. 2017;1860(2):218–26.
34. Xu H, Li Z, Jiang PF, Zhao L, Qu C, Van de Peer Y, Liu YJ, Zeng QY. Divergence of active site motifs among different classes of *Populus* glutaredoxins results in substrate switches. Plant J. 2022;110(1):129–46.
35. Suo J, Zhao Q, Zhang Z, Chen S, Cao J, Liu G, Wei X, Wang T, Yang C, Dai S. Cytological and proteomic analyses of *Osmunda cinnamomea* germinating spores reveal characteristics of fern spore germination and rhizoid tip growth. Mol Cell Proteomics. 2015;14(9):2510–34.
36. Yoo SD, Cho YH, Sheen J. Arabidopsis mesophyll protoplasts: a versatile cell system for transient gene expression analysis. Nat Protoc. 2007;2(7):1565–72.
37. Garg R, Jhanwar S, Tyagi AK, Jain M. Genome-wide survey and expression analysis suggest diverse roles of glutaredoxin gene family members during development and response to various stimuli in rice. DNA Res. 2010;17(6):353–67.
38. Qian Z, Rao X, Zhang R, Gu S, Shen Q, Wu H, Lv S, Xie L, Li X, Wang X, et al. Genome-wide identification, evolution, and expression analyses of AP2/ERF family transcription factors in *Erianthus fulvus*. Int J Mol Sci. 2023;24(8):7102.
39. Zannini F, Moseler A, Bchini R, Dhalleine T, Meyer AJ, Rouhier N, Couturier J. The thioredoxin-mediated recycling of *Arabidopsis thaliana* GRXS16 relies on a conserved C-terminal cysteine. Biochim Biophys Acta. 2019;1863(2):426–36.
40. Fernandes AP, Holmgren A. Glutaredoxins: glutathione-dependent redox enzymes with functions far beyond a simple thioredoxin backup system. Antioxid Redox Signal. 2004;6(1):63–74.
41. Morita S, Yamashita Y, Fujiki M, Todaka R, Nishikawa Y, Hosoki A, Yabe C, Nakamura J, Kawamura K, Suwastika IN, et al. Expression of a rice glutaredoxin in aleurone layers of developing and mature seeds: subcellular localization and possible functions in antioxidant defense. Planta. 2015;242(5):1195–206.
42. Ding S, He F, Tang W, Du H, Wang H. Identification of maize cc-type glutaredoxins that are associated with response to drought stress. Genes. 2019;10(8):610.
43. Malik WA, Wang X, Wang X, Shu N, Cui R, Chen X, Wang D, Lu X, Yin Z, Wang J, et al. Genome-wide expression analysis suggests

glutaredoxin genes response to various stresses in cotton. Int J Mol Sci. 2020;153:470–91.
44. Li T, Li M, Jiang Y, Duan X. Genome-wide identification, characterization and expression profile of glutaredoxin gene family in relation to fruit ripening and response to abiotic and biotic stresses in banana (*Musa acuminata*). Int J Biol Macromol. 2021;170:636–51.
45. Boubakri H, Najjar E, Jihnaoui N, Chihaoui S-A, Barhoumi F, Jebara M. Genome-wide identification, characterization and expression analysis of glutaredoxin gene family (Grxs) in *Phaseolus vulgaris*. Gene. 2022;833:146591.
46. Wang Z, Xing S, Birkenbihl RP, Zachgo S. Conserved functions of Arabidopsis and rice CC-type glutaredoxins in flower development and pathogen response. Mol Plant. 2009;2(2):323–35.
47. Cheng N-H, Liu J-Z, Brock A, Nelson RS, Hirschi KD. AtGRXcp, an Arabidopsis chloroplastic glutaredoxin, is critical for protection against protein oxidative damage. J Biol Chem. 2006;281(36):26280–8.
48. Morton MJL, Awlia M, Al-Tamimi N, Saade S, Pailles Y, Negrão S, Tester M. Salt stress under the scalpel – dissecting the genetics of salt tolerance. Plant J. 2019;97(1):148–63.
49. Rouhier N, Couturier J, Johnson MK, Jacquot JP. Glutaredoxins: roles in iron homeostasis. Trends Biochem Sci. 2010;35(1):43–52.
50. Guo Y, Huang C, Xie Y, Song F, Zhou X. A tomato glutaredoxin gene *SlGRX1* regulates plant responses to oxidative, drought and salt stresses. Planta. 2010;232(6):1499–509.
51. Sharma R, Priya P, Jain M. Modified expression of an auxin-responsive rice CC-type glutaredoxin gene affects multiple abiotic stress responses. Planta. 2013;238(5):871–84.
52. Kumar A, Kumar V, Dubey AK, Ansari MA, Narayan S, Meenakshi, Kumar S, Pandey V, Pande V, Sanyal I. Chickpea glutaredoxin (*CaGrx*) gene mitigates drought and salinity stress by modulating the physiological performance and antioxidant defense mechanisms. Physiol Mol Biol Plants. 2021;27(5):923–44.
53. Ning X, Sun Y, Wang C, Zhang W, Sun M, Hu H, Liu J, Yang L. A rice CPYC-type glutaredoxin *Osgrx20* in protection against bacterial blight, methyl viologen and salt stresses. Front Plant Sci. 2018;9:111.
54. Verma PK, Verma S, Tripathi RD, Pandey N, Chakrabarty D. CC-type glutaredoxin, OsGrx_C7 plays a crucial role in enhancing protection against salt stress in rice. J Biotechnol. 2021;329:192–203.
55. Mieyal JJ, Gallogly MM, Qanungo S, Sabens EA, Shelton MD. Molecular mechanisms and clinical implications of reversible proteins-glutathionylation. Antioxid Redox Signal. 2008;10(11):1941–88.
56. Deponte M. Glutathione catalysis and the reaction mechanisms of glutathione-dependent enzymes. Biochim Biophys Acta. 2013;1830(5):3217–66.
57. Outten CE, Albetel A-N. Iron sensing and regulation in *Saccharomyces cerevisiae*: Ironing out the mechanistic details. Curr Opin Microbiol. 2013;16(6):662–8.
58. Couturier J, Przybyla-Toscano J, Roret T, Didierjean C, Rouhier N. The roles of glutaredoxins ligating Fe–S clusters: Sensing, transfer or repair functions? Biochim Biophys Acta. 2015;1853(6):1513–27.
59. Berndt C, Lillig CH. Glutathione, glutaredoxins, and iron. Antioxid Redox Signal. 2017;27(15):1235–51.
60. Liu X, Liu S, Feng Y, Liu J-Z, Chen Y, Pham K, Deng H, Hirschi KD, Wang X, Cheng N. Structural insights into the N-terminal GIY–YIG endonuclease activity of Arabidopsis glutaredoxin AtGRXS16 in chloroplasts. Proc Natl Acad Sci U S A. 2013;110(23):9565–70.
61. Rey P, Becuwe N, Tourrette S, Rouhier N. Involvement of Arabidopsis glutaredoxin S14 in the maintenance of chlorophyll content. Plant Cell Environ. 2017;40(10):2319–32.
62. Valassakis C, Dervisi I, Agalou A, Papandreou N, Kapetsis G, Podia V, Haralampidis K, Iconomidou VA, Spaink HP, Roussis A. Novel interactions of selenium binding protein family with the PICOT containing proteins AtGRXS14 and AtGRXS16 in *Arabidopsis thaliana*. Plant Sci. 2019;281:102–12.
63. Bohle F, Rossi J, Tamanna SS, Jansohn H, Schlosser M, Reinhardt F, Brox A, Bethmann S, Kopriva S, Trentmann O, et al. Chloroplasts lacking class I glutaredoxins are functional but show a delayed recovery of protein cysteinyl redox state after oxidative challenge. Redox Biol. 2024;69:103015.

Publisher's Note